AIMS Materials Science, 12(5): 1069–1091.
DOI: 10.3934/matersci.2025050
Received: 12 July 2025
Revised: 23 October 2025
Accepted: 06 November 2025
Published: 13 November 2025

https://www.aimspress.com/journal/Materials

Review

Advances in synthesis strategies and multifunctional applications of silicon carbide materials

Aoyi Dong[1], Shaoyi Shen[1], Jialin Wang[1], Xinxin Liu[2], Bibo Han[1], Song Wu[1], Xinhua Zheng[1], Yaguang Sun[1] and Shikai Liu[1,*]

[1] School of Materials Science and Engineering, Henan University of Technology, Zhengzhou 450001, China
[2] Shenzhen Jijia New Material Technology Co., Ltd., Shenzhen 518172, China

* **Correspondence:** Email: shikai_liu@haut.edu.cn; Tel: +86-371-67758737.

Abstract: Silicon carbide (SiC), a leading third-generation wide-bandgap semiconductor, exhibits exceptional electrical, thermal, and mechanical properties, including a high breakdown field, superior thermal conductivity, and remarkable environmental stability, making it indispensable for high-power electronics, high-temperature applications, and advanced composites. This review systematically outlines recent advances in SiC materials, with an emphasis on crystal structure characteristics, innovative synthesis routes, and cross-disciplinary applications. The polytypism of SiC and structure—property correlations governing its band structure and carrier mobility—are elucidated. A comparative analysis is then provided on controllable preparation strategies for micro/nano SiC powders, highlighting emerging eco-friendly and low-temperature synthesis pathways. Furthermore, the mechanisms underlying SiC's performance in structural ceramics, catalytic supports, microwave absorption, and supercapacitors are comprehensively discussed, with particular attention paid to its wide-temperature stability and interface enhancement effects. Finally, prevailing challenges in scalable synthesis and defect control are addressed, along with several promising research directions: (1) defect-engineered quantum sensing platforms; (2) low-carbon manufacturing using biomass-derived carbon sources; and (3) deep integration of SiC power devices with smart grid architectures. This review aims to provide theoretical insights and technical guidance for the multi-scale design and application of SiC materials in the fields of new energy and quantum technologies.

Keywords: silicon carbide; structural modulation; synthesis strategies; interdisciplinary integration

1. Introduction

As a typical covalent compound, silicon carbide (SiC) has emerged as a key candidate for high-performance materials in extreme environments, owing to its high hardness (Mohs hardness 9.5), excellent corrosion resistance, extremely low coefficient of thermal expansion (4.5×10^{-6} °C^{-1}, and wide bandgap characteristics (3C-SiC: 2.2 eV; 4H-SiC: 3.26 eV) [1,2]. In traditional industrial applications, SiC has been widely used as an abrasive and refractory material. Low-grade SiC powders (purity ≥85%) enhance steelmaking efficiency and product quality in metallurgical deoxidation processes [3,4]. In functional ceramics, SiC-based ballistic armor, satellite mirror coatings, and high-temperature oxidation-resistant components have further expanded its applications in defense and aerospace engineering [3–5]. Recently, with the rapid development of new energy and information technologies, the wide-bandgap semiconductor properties of SiC have been extensively explored. Its breakdown field strength (4H-SiC: 2.5 MV/cm) and thermal conductivity (4.5 W/cm K) significantly exceed those of conventional silicon-based materials, driving the commercialization of SiC metal-oxide-semiconductor field-effect transistor (MOSFETs) and diodes in smart grids, new energy vehicles, and 5G communication systems [5,6].

However, the large-scale application of high-performance SiC devices still faces two critical challenges. First is the controllable synthesis of micro/nano powders. The growth of semiconductor-grade SiC single crystals requires raw materials with a purity exceeding 99.9995% to minimize dislocation defects [7,8], while aerospace composite materials demand nano-sized SiC powders (particle size <100 nm) to achieve interfacial enhancement [9]. The second is polytype control and defect engineering. The distinct bandgap structures of different polytypes (e.g., 3C/4H/6H-SiC) directly affect device performance [10,11], and stacking faults and micropipe defects during single-crystal growth severely limit wafer yield [12]. Thus, developing high-purity SiC micro/nano powders with controlled polytypes and uniform particle sizes, along with establishing precise structure–property–application correlations, has become the core objective of current research.

This review systematically examines the advancements in SiC materials from an integrated perspective of materials science and engineering applications. Unlike previous reviews that often focus on a single domain, this work emphasizes the interdisciplinary linkages between synthesis strategies, structural control, and performance across diverse fields. Specifically, it aims to provide a critical analysis of (1) the mechanistic correlation between polytypism and multi-field properties, (2) eco-friendly and low-temperature synthesis pathways for scalable production, and (3) the underlying mechanisms of SiC in emerging applications such as microwave absorption, supercapacitors, and quantum sensing platforms.

Furthermore, this review proposes several forward-looking strategies to address existing challenges, including defect engineering for quantum devices, low-carbon manufacturing using biomass-derived carbon sources, and the deep integration of SiC power devices with smart grid systems. By synthesizing the latest multidisciplinary research, this work not only offers a theoretical framework but also outlines a technological roadmap for the multi-scale design and application of SiC materials in the fields of new energy and quantum technology.

2. Overview of silicon carbide

2.1. Crystal structure and polytypic characteristics

SiC, a binary compound semiconductor composed of silicon (Si) and carbon (C) atoms linked by strong covalent bonds (bond length: 1.89 Å; bond energy: 447 kJ/mol), features a three-dimensional close-packed network of alternating SiC_4 and CSi_4 tetrahedra [13]. As illustrated in Figure 1, Si and C atoms occupy tetrahedral centers, achieving stable electronic configurations via sp^3 hybridization, while adjacent tetrahedra form layered stacking structures through edge- and vertex-sharing [14]. This unique crystalline architecture grants SiC remarkable polytypism: over 200 polytypes (e.g., 3C-SiC, 4H-SiC, 6H-SiC) have been identified under varying temperature and pressure conditions, arising from differences in stacking sequences along the [111] direction (cubic zinc blende structure) or [0001] direction (hexagonal wurtzite structure) [15]. Notably, 3C-SiC (β-phase, with ABC periodic stacking) crystallizes in the cubic system, whereas 4H/6H-SiC (α-phase, with ABCB/ABCACB stacking) belongs to the hexagonal system. Critical physical properties, including band structure, carrier mobility, and thermal conductivity, are directly determined by these stacking configurations. For example, the wider bandgap of 4H-SiC (3.26 eV) compared to 3C-SiC (2.2 eV) makes it more suitable for high-power semiconductor devices [16].

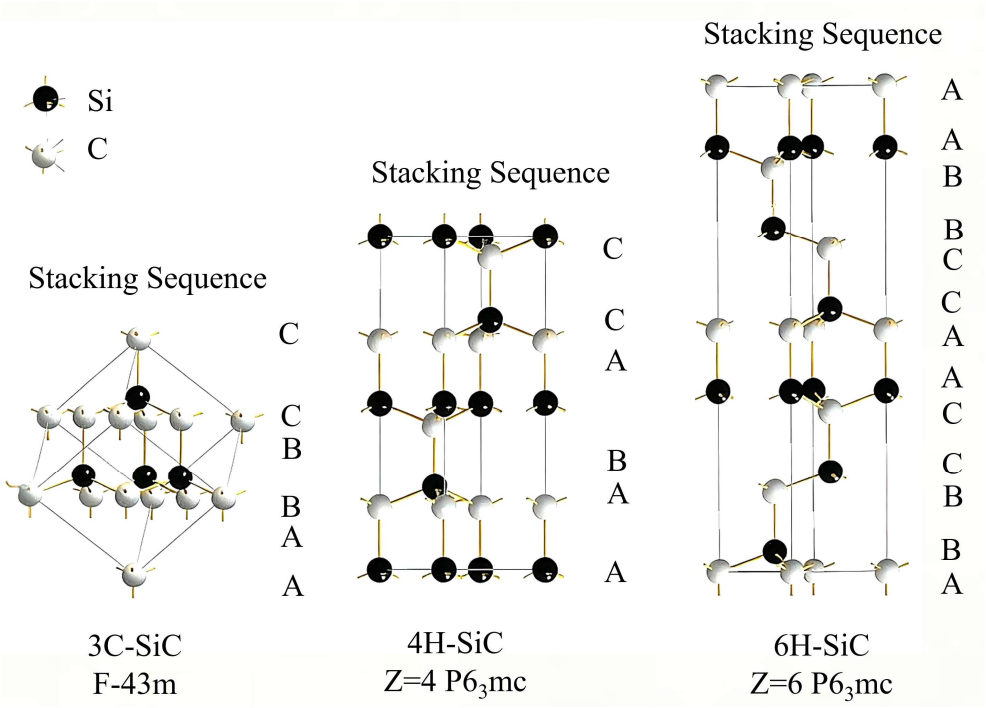

Figure 1. Schematic of stacking structures in silicon carbide polytypes. Black spheres: Si; white spheres: C; A/B/C denote stacking sequences.

2.2. Physicochemical properties and functional advantages

SiC exhibits exceptional properties owing to its strong covalent bonding and polytypic tunability (Table 1). These advantages are primarily reflected in three key aspects:

(1) Extreme environmental stability: SiC possesses a high melting point (>2700 °C), low thermal expansion coefficient (4.5×10^{-6} °C^{-1}), and exceptional oxidation resistance (onset temperature >1600 °C). These properties establish SiC as an ideal material for high-temperature refractories and aerospace coatings [17,18].

(2) Semiconductor characteristics: with its wide bandgap (3C-SiC: 2.2 eV; 4H-SiC: 3.26 eV), high breakdown electric field (4H-SiC: 2.5 MV/cm), and superior thermal conductivity (~4.9 W/cm·K for 4H-SiC at 300 K), SiC significantly outperforms silicon (Si). This enables stable device operation under extreme conditions such as high temperature (>600 °C), high frequency (>100 kHz), and high voltage (>10 kV) [19,20].

(3) Mechanical performance: SiC combines high hardness (Mohs hardness 9.5), outstanding wear resistance, and excellent thermal conductivity (e.g., ~120 W/m K near room temperature (RT)). This synergy yields superior performance in demanding structural ceramic and composite applications [21].

Table 1. Comparison of key electrical parameters between silicon and silicon carbide polytypes.

Property	Si	3C-SiC	4H-SiC	6H-SiC
Bandgap energy (eV)	1.12	2.2	3.26	3
Relative dielectric constant	11.9	9.6	9.7	9.8
Electron mobility ($cm^2/V·S$)	1350	1000	500	950
Electron saturation velocity (10^7 cm/s)	1.1	2	2	2
Hole mobility ($cm^2/V·S$)	420	40	120	40
Critical breakdown electric field (MV/m)	0.3	1.2	2.5	2.4
Thermal conductivity (W/cm·k)	1.5	4.5	4.5	4.5

Based on applications, SiC materials can be categorized into two main types:

(1) Polycrystalline SiC: existing in ceramic forms, it exhibits high strength (flexural strength >400 MPa) and corrosion resistance, making it suitable for high-temperature kiln furniture, ballistic armor, and related applications [21].

(2) Single-crystal SiC: as a cornerstone material for third-generation semiconductors, its low on-resistance (<5 mΩ·cm^2) and high switching efficiency (70% reduction in switching losses) drive innovations in power devices for new energy vehicles and 5G communication systems [9,16,22].

3. Research progress in silicon carbide synthesis

The expanding applications of SiC have spurred progress in its synthesis techniques from conventional solid-phase reactions to precise nanoscale synthesis. Currently, the primary synthesis routes include solid-phase, liquid-phase, and vapor-phase methods, differentiated by their reaction media. This section systematically discusses each methodology, focusing on three key aspects: technical principles, process characteristics, and recent progress.

3.1. Solid-phase methods

Solid-phase methods synthesize SiC powders directly via high-temperature solid-state reactions. These approaches benefit from well-established processes and are cost-effective but constrained by diffusion kinetics, typically yielding micrometer-scale particles [23–25]. Representative techniques include:

(1) Carbothermal reduction

The conventional synthesis of SiC typically employs silicon dioxide (SiO_2) and a carbon source (e.g., coke or biomass-derived carbon) as raw materials, which react at 1500–2000 °C according to the reaction $SiO_2 + 3C \rightarrow SiC + 2CO\uparrow$. This method is mainly used for producing industrial-grade SiC powders with a purity of approximately 85%–95% [23]. In recent years, the recycling and valorization of industrial waste materials have become a research hotspot. For instance, Gao et al. [24] utilized silicon slurry cutting waste (composed primarily of Si, SiO_2, SiC, and Fe_xO_y) as the silicon source, petroleum coke as the carbon source, and NaCl as an additive. A series of variable experiments was conducted to investigate the effects of Fe impurities, NaCl dosage, and smelting temperature on SiC synthesis. The results revealed that Fe acts as a catalyst to promote SiC formation at lower temperatures; however, excessive Fe leads to the formation of Si–Fe alloys, thereby reducing the product purity. The introduction of NaCl facilitates impurity removal by forming and volatilizing $FeCl_2$, while its melting and evaporation behavior enhances heat and mass transfer. Thermodynamic analysis indicated that the reaction becomes feasible when the temperature exceeds 1500 °C, and at 1850 °C, the obtained SiC achieved a purity exceeding 93 wt.%. Petroleum coke and pre-existing SiC particles served as dual nucleation centers, and maintaining a C/Si ratio above 3 ensured phase stability, achieving the waste-free recycling of silicon slurry cutting waste. In another study, Lu et al. [25] employed semi-coke from waste tires and quartz sand as starting materials. After mixing and drying to remove moisture, the mixture was subjected to a tubular furnace reaction to produce SiC-containing intermediates, followed by oxidation in a muffle furnace to remove residual impurities and obtain the final SiC product (Figure 2). The study examined the influence of raw material particle size on the phase composition, morphology, particle size, and reaction extent of SiC. It was found that smaller semi-coke particles with larger specific surface areas promoted gas–solid reactions, facilitated uniform SiC nucleation and growth, reduced whisker and secondary particle formation, and improved crystal integrity. Conversely, larger quartz sand particles slowed the conversion of solid-phase SiO_2 to gaseous SiO, thereby minimizing SiO volatilization losses and maintaining a continuous reaction, resulting in higher SiC crystallinity and yield. Through the identification of the intermediate SiO species and analysis of the C/Si ratio, the formation mechanism of SiC particles was confirmed to follow a gas–solid reaction, while the whisker formation was attributed to a gas–gas reaction process.

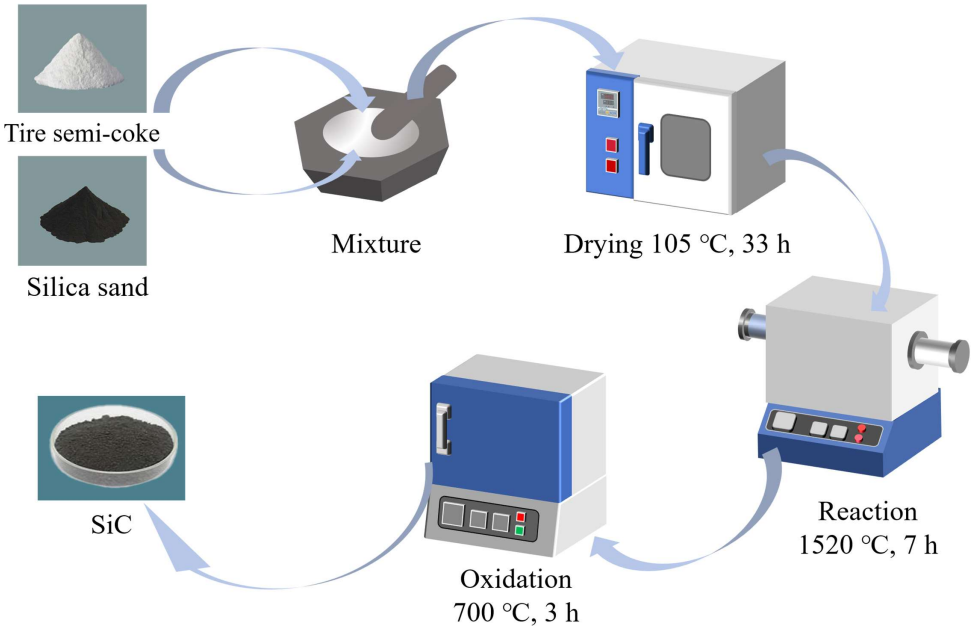

Figure 2. Flowchart for SiC preparation.

(2) Combustion synthesis (CS)

CS is a high-temperature technique that utilizes the exothermic heat generated by the reactants themselves to sustain the reaction. Owing to its short reaction duration, simple setup, and low energy consumption, CS has been widely employed for the synthesis of nanoscale ceramic powders. Depending on the reaction mode, CS can be categorized into three main types: self-propagating high-temperature synthesis (SHS), volume combustion synthesis (VCS), and solution combustion synthesis (SCS). Alexander S. Mukasyan and co-workers synthesized β-SiC nanopowders using Si and graphite powders as raw materials. The powders were first subjected to short-duration high-energy ball milling (HEBM) pretreatment, followed by SHS under an inert atmosphere [26]. The analysis revealed that HEBM significantly increased the contact area between Si and C and removed surface oxide layers, thereby enhancing the reaction activity. This enabled the weakly exothermic Si–C system to achieve self-sustaining combustion. During the combustion stage, molten Si reacted with solid C via a liquid–solid mechanism, and the resulting SiC inherited the composite morphology of the milled Si/C precursors. This approach provided a kinetic pathway for additive-free synthesis of uniform and high-purity SiC nanopowders. Kirakosyan et al. [27] developed a two-step solution combustion synthesis–high-speed temperature scanning (SCS–HSTS) method. Using ammonium nitrate as an oxidizer, a homogeneous SiO_2–C precursor was first produced via SCS. The mixture was then rapidly heated to 1600 °C at a rate of 300 °C/min. At 1440 °C, SiO_2 underwent carbothermal reduction with carbon to form SiC-Al_2O_3 fibers, which acted as nucleation centers to guide the oriented growth of SiC whiskers, elucidating the role of nucleation sites in controlling SiC crystal morphology. Han et al. [28] synthesized SiC using Si powder and polytetrafluoroethylene (PTFE), where PTFE functioned simultaneously as a carbon source and gasifying agent. The formation of SiC proceeded through a three-stage combustion process: (i) low-temperature reaction between Si and PTFE to form intermediates; (ii) intermediate-temperature reaction between gaseous SiF_2 and carbon; and (iii) high-temperature reaction between gaseous Si and carbon (Figure 3). The evolution of gaseous

by-products induced volumetric expansion, forming a highly porous structure. The combustion front propagated at a rate of 30 cm/s, reaching 1800 °C within 4 s. The rapid reaction inhibited excessive grain growth, yielding SiC aerogels with an ultralow density of 12 mg/cm^3 and a porosity of 99.6%, offering an efficient and low-cost route for large-scale SiC aerogel production. In another study, the same group introduced a dual thermal-compensation mechanism by coupling the strongly exothermic Si–N_2 (ΔH = –736 kJ/mol) and weakly exothermic Si–C systems. The heat released from the Si–N_2 reaction increased the system temperature above 1100 °C, initiating the Si–C combustion, while the Si–C reaction absorbed excess heat, preventing Si melting. The CO generated in situ created a reducing atmosphere, lowering the oxygen content of Si_3N_4 to 0.46 wt%. The combustion front propagated at 17–25 mm/min, leading to the simultaneous formation of 30 nm SiC nanoparticles and high-purity Si_3N_4 powders. This coupling strategy successfully achieved thermodynamic and kinetic synergy between two ceramic systems, establishing a new paradigm for the co-synthesis of multiphase ceramic materials [29].

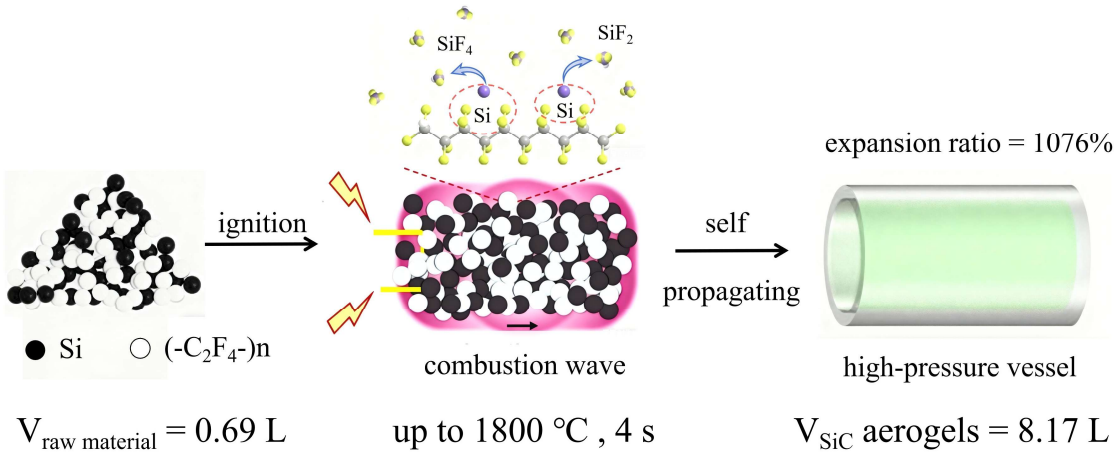

Figure 3. Schematics for the flash synthesis of SiC aerogels.

Bio-template method: the bio-template method utilizes natural biomass materials (e.g., rice husk and wood) as renewable carbon and silicon sources to synthesize porous SiC through carbonization–silicification reactions. This strategy combines biomimetic structural replication with sustainability advantages, offering a cost-effective and environmentally friendly approach for SiC production [30–32]. Alweendo et al. [33] employed rice husk as the raw material without using catalysts. After cleaning, drying, and varying pretreatments (raw, hand-milled, and ball-milled), the samples were first carbonized at 700 °C to form amorphous carbon and then subjected to carbothermal reduction in an argon atmosphere. The obtained products were purified via calcination and acid leaching (HF/HCl). The ball-milled sample, exhibiting a larger specific surface area, achieved the highest SiC yield (69.2%) at 1500 °C after 120 min. The products consisted of whiskers and particles, with SiC formation governed by a gas–solid mechanism. Enhanced SiO diffusion and uniform nucleation on carbon surfaces were promoted by increased surface area, while the inert atmosphere stabilized the β-SiC phase by preventing oxidation. This study demonstrated a simple and catalyst-free route to synthesize high-yield SiC and elucidated the effects of process parameters on yield and morphology, contributing to the valorization of rice husk resources. Kieu Do et al. [34] further

incorporated silica gel—prepared from sodium silicate and acetic acid—as an additional silicon source, leveraging the inherent Na_2O in rice husk as a catalyst. SiC was synthesized via combustion under a CO_2 atmosphere at 800–1300 °C (Figure 4). The SiC content increased with temperature up to 1200 °C (20.4%) but slightly decreased at 1300 °C (18.6%) due to oxidation. Both α- and β-SiC phases were observed, with β→α transformation occurring at higher temperatures. Na_2O effectively reduced the melting point and viscosity of SiO_2, lowering the SiC formation onset to 800 °C and promoting phase transformation, while CO_2 maintained carbon stability at low temperatures and enhanced oxidation at high temperatures. This approach overcame the limitation of low silicon content in rice husks and provided a sustainable pathway for converting agricultural residues into high-value SiC materials, contributing to green synthesis and circular utilization of biomass.

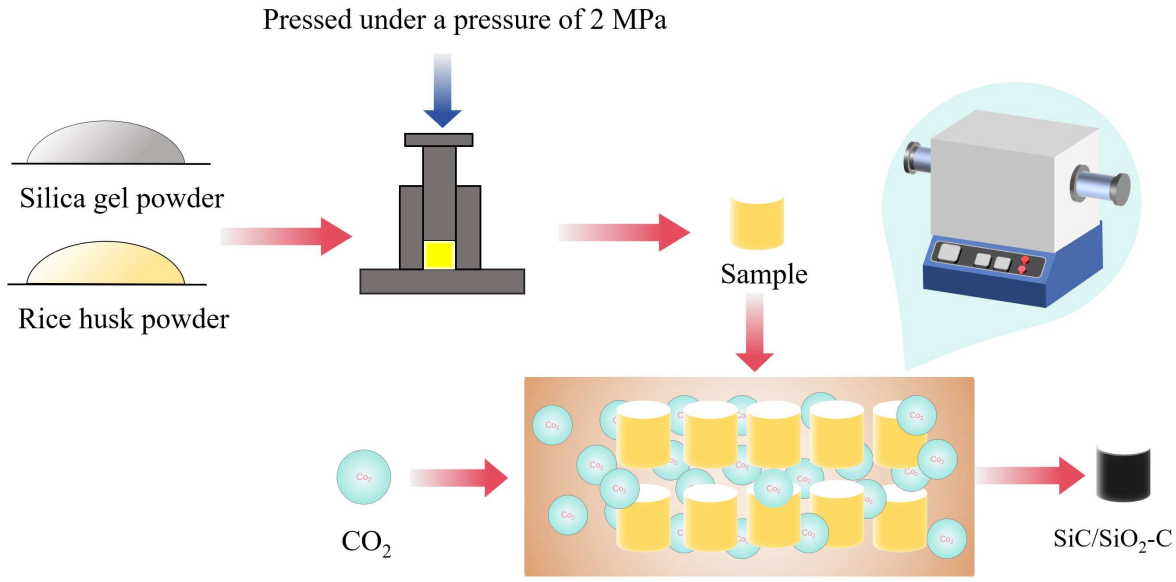

Figure 4. Diagram of the prototyping process.

Although biomass-derived carbon sources show great potential for sustainable low-carbon manufacturing of semiconductors such as SiC, challenges remain due to the compositional complexity of precursors, poor controllability during carbonization, and impurity residues, which hinder stability and scalability. Moreover, their electrical and interfacial properties require further optimization. Future efforts should focus on precursor standardization, controllable carbonization mechanisms, and interfacial engineering with semiconductors, assisted by machine learning and in situ characterization to achieve green and efficient low-carbon manufacturing.

3.2. Liquid-phase methods

Liquid-phase methods enable controlled synthesis of nano-SiC using solution- or molten salt-based media, offering enhanced uniformity and precise morphology control. These techniques fall into two primary categories:

(1) Sol–gel method

The sol–gel method synthesizes SiC nanoparticles through the hydrolysis–condensation reaction of precursors such as tetraethyl orthosilicate (TEOS) and phenolic resins, forming homogeneous sols followed by carbothermal reduction at elevated temperatures. Li et al. [35] employed TEOS and linear phenolic resin as raw materials, using oxalic acid (OA) and hexamethylenetetramine (HMTA) as dual catalysts in a two-step sol–gel process to prepare phenolic resin–SiO_2 hybrid gels. Subsequent vacuum carbothermal reduction at 1650 °C for 30 min yielded β–SiC powders. The mechanism involved OA-catalyzed hydrolysis of TEOS and HMTA-catalyzed condensation and resin curing, with an optimal OA/TEOS molar ratio ensuring matched reaction rates for uniform nucleation. The carbothermal conversion followed the SiO_2→SiO (g)→SiC pathway, where the vacuum environment and high temperature ensured complete reaction. This catalyst-free and controllable process provided thermodynamic and kinetic guidance for producing high-purity SiC powders. Najafi et al. [36] used TEOS, trimethyl borate (TMB), and phenolic resin with ammonium polycarboxylate (APC) as a dispersant to prepare SiC–B_4C composite nanopowders via a co-hydrolysis–condensation process. Partial hydrolysis of TEOS followed by TMB addition enabled hetero-condensation and Si–O–B bond formation, achieving molecular-level mixing. Under mildly acidic conditions (pH 3–4), APC suppressed particle agglomeration by electrostatic repulsion, yielding precursor particles <10 nm. Upon heating at 1350 °C, Si–O and B–O bonds simultaneously reacted with carbon to form β–SiC (cubic) and B_4C (rhombohedral), overcoming the inhomogeneity of traditional mechanical mixing and offering a strategy for multi-component carbide synthesis (Figure 5). Moreover, a microwave-assisted approach further enhanced synthesis efficiency: silicon carbide-titanium dioxide (SiC-TiO_2) core-shell nanoparticles were synthesized via a sol-gel method [37]. Microwave treatment enabled the crystallization of TiO_2 into the anatase phase at a temperature of 190 ± 10 °C, which is significantly lower than the 450 °C required for conventional furnace heating.

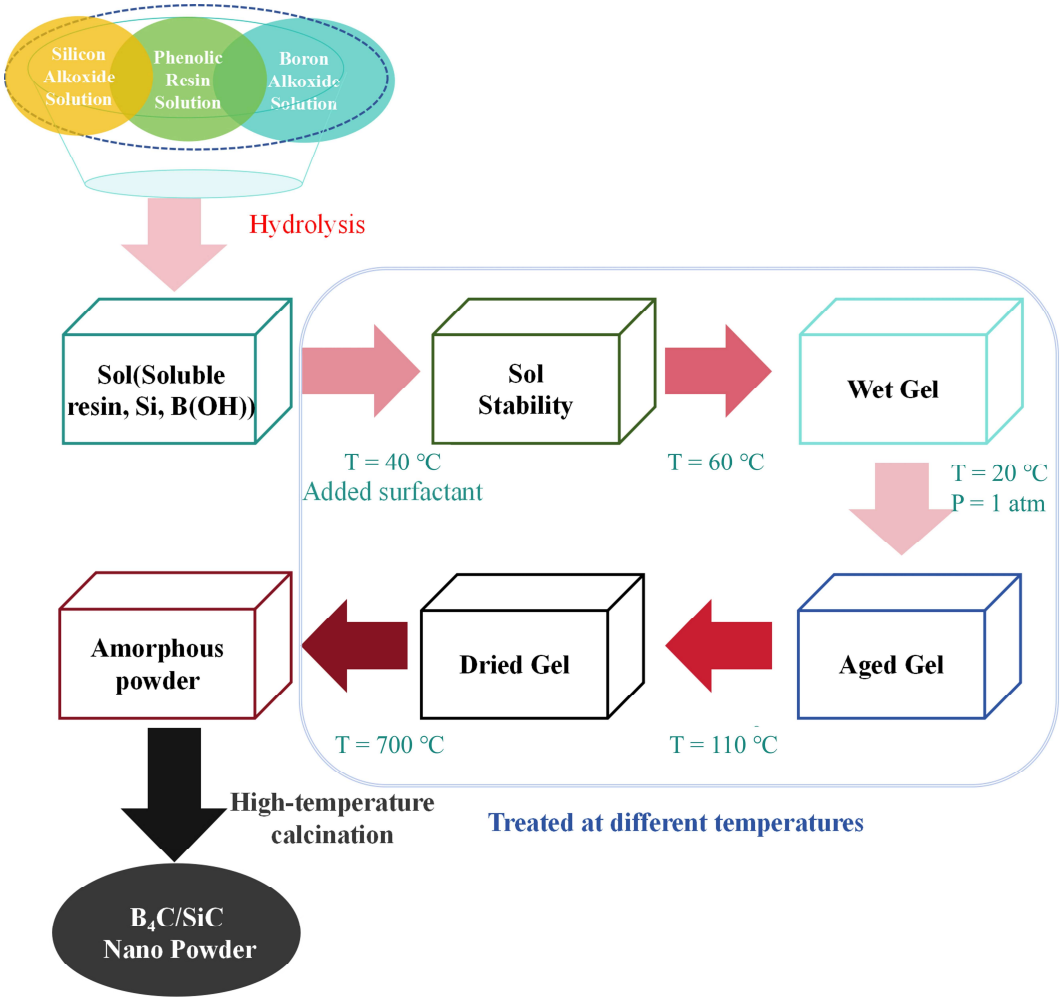

Figure 5. Flowchart of experimental procedure.

(2) Molten salt method

In recent years, molten salt–assisted synthesis has emerged as an effective strategy for achieving low-temperature and morphology-controlled fabrication of SiC, owing to its unique ionic environment and enhanced mass transport properties. By introducing dissolution–diffusion–precipitation or chemical–electrochemical coupling mechanisms within low-melting-point salt media, this approach not only significantly reduces reaction temperatures but also enables precise control over crystal phase evolution and microstructural features. Xie et al. [38] demonstrated the self-assembly of 3C–SiC nanorods on multi-walled carbon nanotube templates within a NaCl–NaF molten salt system, where the dissolution and diffusion of Si facilitated anisotropic growth at 200–250 °C, lower than conventional gas–solid methods. This work highlights the critical role of molten salts in promoting silicon migration and oriented crystal growth. Wang et al. [39] further employed lignin–phenolic resin as a carbon source to generate molten catalysts during pyrolysis in situ, achieving vapor–liquid–solid growth of β–SiC nanowires (~1100 °C). The resulting nanowires exhibited high crystallinity and large specific surface area, making them promising candidates for catalytic applications. Moreover, Pang et al. [40] developed an electrochemical–carbothermal hybrid mechanism within a $CaCl_2$ molten salt system, enabling direct carbothermal conversion of SiO_2/C mixtures into polycrystalline 3C–SiC nanoparticles (8–14 nm) at only 900 °C. The process involves simultaneous electro-deoxidation and

in situ carburization, featuring low energy consumption and yielding SiC with distinct quantum confinement effects, which are advantageous for optoelectronic applications. Overall, molten salt–assisted synthesis offers a versatile and energy-efficient route for tailoring SiC morphology, structure, and functionality, providing new insights and methodologies for the controlled preparation of high-performance SiC nanomaterials.

3.3. Gas-phase methods

Gas-phase methods synthesize target products by converting precursors into the gas phase—either directly or through precursors—allowing chemical reactions to occur homogeneously, followed by condensation. While these methods enable the production of high-quality silicon carbide powders with precise composition control, they face limitations including high operating costs, low yields, and challenges in scaling for industrial production. Notable approaches include:

(1) Laser-induced method

Developed in the late 20th century, this method synthesizes nano-SiC through resonant laser irradiation of reactive gases or catalyst molecules. Under laser irradiation, gases undergo photolytic or pyrolytic reactions. Nucleation and growth of ultra-fine particles are promoted by optimizing process parameters, yielding nanoscale SiC particles. For example, Fedorov et al. [41] formed SiC coatings on silicon substrates using an ethylene/argon atmosphere, achieving rapid surface transformation with high spatial resolution (<0.5 mm) and minimal thermal impact zones.

(2) Chemical vapor deposition (CVD)

Dense β-SiC coatings are deposited using methyltrichlorosilane (MTS, CH_3SiCl_3) with H_2-N_2 precursors at 1100–1400 °C. Wu et al. [42] demonstrated that SiC coatings were deposited on C/C composite substrates via cold-wall CVD using hexamethyldisilylamine as the precursor and N_2 as the carrier gas within the deposition temperature range of 1010–1220 °C; the coating exhibited a single β-SiC (3C) phase at 1010, 1060, 1100, and 1220 °C, coexisted with α-SiC (2H) and β-SiC (3C) phases at 1130 and 1180 °C, and its surface morphology transformed from smooth with spherical particles to rough "cauliflower-like" structures as temperature increased, while the deposition rate rose from 5.9 to 60.5 $\mu m \cdot h^{-1}$, forming a compact coating with good interfacial structure.

(3) Plasma-assisted vapor synthesis

Under electric fields, gas ionization generates plasma, which discharges to activate and react with gaseous species for chemical vapor deposition. Bertran et al. [43] fabricated nanostructured ns-Si:H/ns-SiC:H multilayer ceramic coatings embedded with SiC nanoparticles on c-Si substrates via modulated rf plasma chemical vapour deposition (PECVD) using SiH_4-CH_4-Ar gaseous mixtures, characterized their structure by transmission electron microscopy (TEM), selected area electron diffraction (SAED), Fourier Transform infrared spectroscopy (FTIR) and mechanical properties by nanoindentation and pin-on-disc tests, and found that the coatings possess improved hardness, wear resistance, crack propagation resistance and atmospheric stability, showing potential applications in protective coatings, optical fibres and other fields.

The above content reviews the main synthesis methods of SiC, which are categorized by reaction medium into three major types—solid-phase, liquid-phase, and gas-phase methods—covering their technical principles, process characteristics, and recent advances. Solid-phase methods synthesize SiC powders through high-temperature solid-state reactions, featuring mature processes and relatively low costs, but are limited by diffusion kinetics. Liquid-phase methods enable the controllable synthesis of

nano-SiC using solution or molten salt media, with superior product uniformity and morphology tunability. Gas-phase methods produce high-purity SiC via gas-phase conversion of precursors, allowing precise control over composition; however, they are plagued by high costs, low yields, and challenges in large-scale production. Key parameters of SiC synthesis methods are summarized in Table 2.

Table 2. Comparative summary of key parameters in synthesis methods.

Method category		Operating temperature (°C)	Particle size control	Scalability	Environmental impact
Solid phase	Carbothermal reduction	1500–2000	20 nm to 5 μm	High (industrial)	Moderate (waste valorization, but high energy, CO emissions)
	Combustion synthesis	>1400 (rapid)	20–80 nm	Moderate	Low–moderate (exothermic, efficient)
	Bio-template method	800–1300	Nanofibers/particles	Moderate-high	Low (biomass-based, renewable)
Liquid phase	Sol–gel method	600–1400	20–50 nm	Moderate	Low–moderate (organic precursors, recyclable solvents)
	Molten salt method	800–1400	8–100 nm (wires/rods)	Moderate-high	Moderate (reusable salts, lower energy)
Gas phase	Laser-induced method	Variable (laser-based)	Nanoscale	Low	Moderate–high (energy-intensive)
	CVD	600–2200	10–30 nm (films/nano)	Moderate (for films)	Moderate (gas emissions, controllable)
	Plasma-assisted vapor synthesis	>2000 (plasma)	Tens of nanometers	Moderate	High (energy use, byproducts)

4. Applications of SiC

SiC, an advanced structural and functional ceramic material, has become a critical engineering material due to its covalent-bonded crystal structure and polytypic characteristics like 3C-, 4H-, and 6H-SiC [2,9]. Its exceptional physicochemical stability under extreme conditions, combined with outstanding high-temperature strength, low thermal expansion coefficient, ultra-high hardness, and superior wear-corrosion resistance, enables critical applications in aerospace, energy-chemical industries, and defense. Notably, SiC has evolved beyond traditional high-temperature structural uses into a multifunctional platform with applications including composite reinforcement, catalyst supports, microwave-absorbing materials, supercapacitors, and quantum devices (Figure 6).

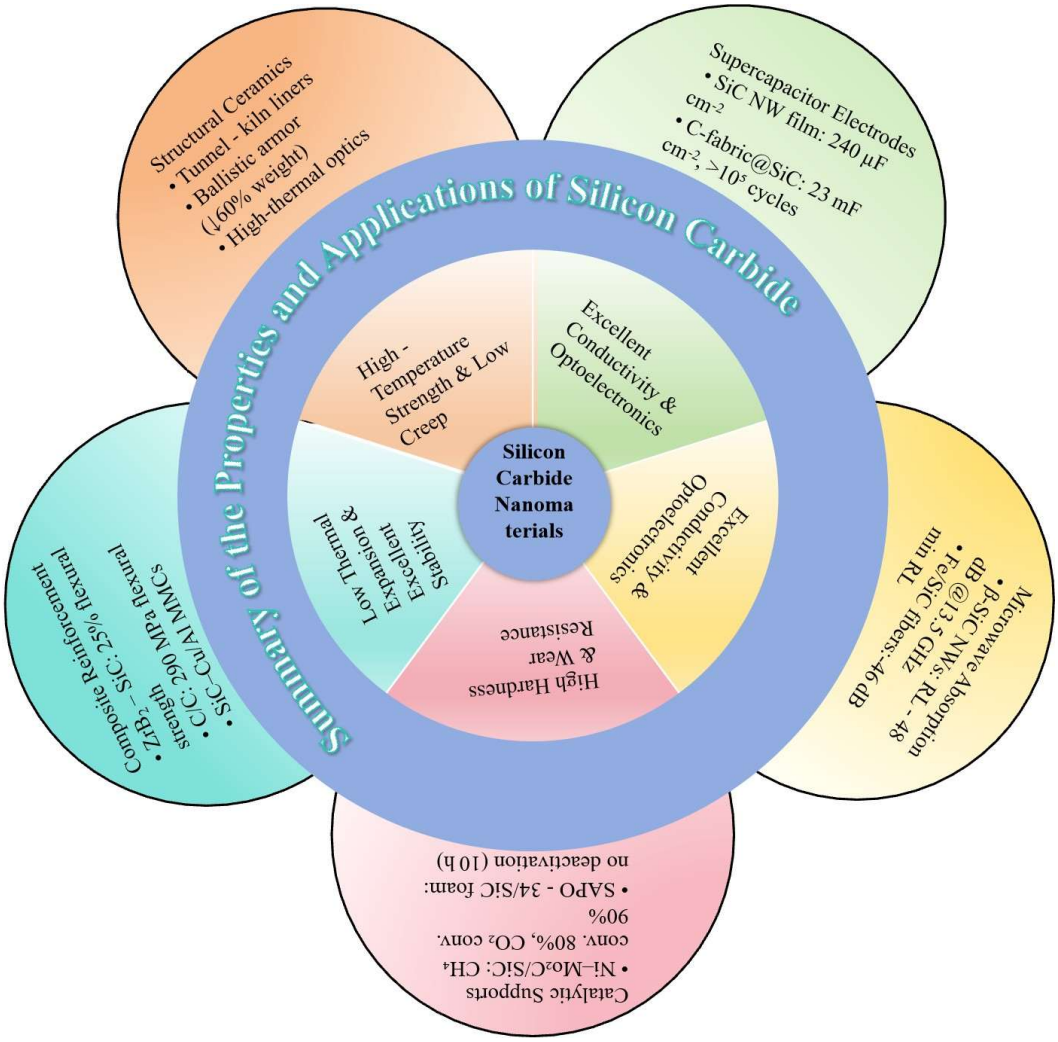

Figure 6. Summary of the properties and applications of silicon carbide.

4.1. Silicon carbide ceramics

As a structural ceramic material, silicon carbide exhibits superior properties compared to metallic structural materials, including high temperature strength, low thermal expansion coefficient, exceptional wear resistance, strong corrosion resistance, high hardness, and minimal high-temperature creep. These characteristics enable it to serve as a critical component in extreme environments, finding significant applications in safety protection, aerospace, machinery, metallurgy, chemical engineering, and electronics [44]. For example, SiC ceramics are used as high-temperature materials in tunnel kilns and shuttle kilns, as well as in wet metallurgical stirring devices, pressurized leaching flash systems, and high-temperature pipelines for hydrochloric acid–based alumina production [45].

Additionally, owing to its hardness—second only to diamond and cubic boron carbide—SiC is widely employed in high-performance ballistic armor. Lightweight ceramic composite armors, consisting of SiC ceramic panels and advanced composite backplates, reduce mass by more than 60% while remaining cost-effective. Innovations such as monolithic SiC multi-curved ballistic inserts further highlight its versatility [46].

4.2. Composite materials

SiC nanomaterials, with their high strength, thermal stability, low coefficient of thermal expansion, and excellent oxidation resistance, have proven to be ideal reinforcements for polymer, ceramic, and carbon/carbon-based composites.

To enhance the flexural strength of composites, Liu et al. [47] incorporated SiC nanoparticles into ZrB_2. Their study revealed that SiC nanoparticles significantly reduced the grain size of ZrB_2; however, excessive addition led to particle aggregation and stress concentration, thereby degrading mechanical properties. Mikociak et al. [48] introduced SiC nanoparticles into carbon/carbon (C/C) composites, and with optimized nanoparticle ratios, they achieved an increase in flexural strength from 120 to 290 MPa and in thermal conductivity from 32 to 53 W/(m·K).

SiC nanoparticles also serve as effective reinforcements for lightweight, high-strength metal matrix composites. Efe et al. [49] demonstrated that adding SiC nanoparticles to copper (Cu) improved its hardness (positively correlated with SiC content) while reducing its density. Zhu et al. [50] synthesized SiC-reinforced Al6802 composites via squeeze casting (SC) and gravity casting (GC), observing enhanced tensile strength, yield strength, and elongation regardless of the casting method.

Bazzar et al. [51] developed polyimide/SiC nanocomposites through in situ polymerization. The resulting poly(triazole-imide)/SiC films exhibited a tensile strength increase from 108 to 165 MPa and high thermal stability (5% weight loss temperature at 500 °C, compared to 380 °C for pure polyimide).

4.3. Catalytic applications

SiC's thermal stability, electrical conductivity, low thermal expansion coefficient, and robust chemical resistance make it an ideal inert support for catalytic applications. As a catalyst support, SiC enhances the performance and stability of active phases compared to traditional supports such as SiO_2 and Al_2O_3 [52].

Silva et al. [53] compared Ni-Mo_2C catalysts supported on Al_2O_3, SiO_2, and SiC. The SiC-supported catalysts achieved 80% CH_4 and 90% CO_2 conversions while minimizing carbon filament formation. Elamin et al. [54] synthesized SAPO-34/SiC foam composites via microwave-assisted methods, yielding catalysts with 2 μm particles (compared to 10–20 μm for ZSM-5) and superior stability in methanol conversion. For hydrogen production, Park et al. [55] developed Ni nanoparticles with Co-modified SiC/$MgAl_2O_4$ supports (NCMAS), which exhibited enhanced activity and stability in propane steam reforming.

4.4. Microwave absorption

Stacking faults in SiC crystals induce strong interfacial dipole polarization, disrupting charge balance and enhancing electromagnetic wave attenuation [56]. One-dimensional SiC materials, with high specific surface area and tunable electrical properties, hold promise for applications in military stealth and radar absorption.

Hu et al. [57] synthesized bamboo-like 3C-SiC nanowires with dense defects via molten salt calcination. A 1.9-mm-thick β-SiC nanowire (NW)/paraffin composite achieved a minimum reflection loss (RL) of −48.13 dB at 13.52 GHz, with an effective bandwidth of 2.56 GHz. Chiu et al. [58] reported dual-band absorption (−31.7 dB at 8.3 GHz and −9.8 dB at 2.7 GHz) in 35 wt% β-SiC

NW/epoxy composites. Hou et al. [59] fabricated Fe/SiC hybrid fibers via electrospinning and pyrolysis, which achieved an RL of −46.3 dB at a PCS/Fe ratio of 3:0.5.

4.5. Supercapacitors

SiC exhibits unique advantages in micro- and high-power supercapacitor electrodes due to its wide bandgap, high thermal conductivity, strong chemical stability, and mechanical strength. Different polytypes (3C, 4H, 6H), dimensions (0D, 1D, 2D, 3D), and morphologies (porous structures, nanosheets, nanoflowers) affect its effective specific surface area, electrolyte wettability, and electron/ion transport pathways, thus directly regulating the power density and cycle life of the devices [60]. At the microscopic mechanism level, the charge storage performance of SiC is highly dependent on defect states and surface functional groups. For example, defects such as silicon vacancies, carbon vacancies, and stacking faults can introduce intermediate states in the bandgap, thereby increasing electron injection/transport rates, providing additional pseudocapacitive sites, and enhancing energy storage performance [61]. On the other hand, surface oxygen/nitrogen functionalization (e.g., –OH, –O–, N-doping) can improve the hydrophilicity of the electrode and the wettability of electrolyte ions, strengthen the adsorption and desorption of ions in pores/surfaces, and enhance the contribution of electric double-layer capacitance [62]. Based on these two mechanisms, SiC-based electrodes can achieve high cycle stability and high-rate performance even in high-temperature and harsh environments, providing a feasible path for next-generation supercapacitor materials [63].

Specifically, two-dimensional nanowire structures provide a high aspect ratio and large specific surface area, which can effectively shorten ion diffusion paths and improve electron transport rates, thereby enhancing electric double-layer capacitance performance. Alper et al. [64] synthesized SiC nanowire films via chemical vapor deposition and achieved a specific capacitance of 240 $\mu F \cdot cm^{-2}$, which is comparable to that of carbon-based electrodes. Meanwhile, heterostructures constructed by compounding SiC with conductive carbon (e.g., graphene), metal oxides, or MnO_2 can further improve specific capacitance and energy density through interface electron/ion coupling, enhanced hydrophilicity, and increased active sites. Gu et al. [65] prepared flexible electrodes using SiC nanowires grown on carbon fiber fabrics as active materials, which exhibited a specific capacitance of 23 $mF \cdot cm^{-2}$ (in contrast, the specific capacitance of pure fabrics was 1.2 $mF \cdot cm^{-2}$) with no capacitance loss after 10^5 charge-discharge cycles. Future research should focus on precisely controlling defect types/concentrations and surface chemical states to balance conductivity, self-discharge behavior, and cycle life, thereby achieving synchronous improvement in high energy density and high-power density of SiC supercapacitors.

4.6. Other applications

SiC nanoparticles exhibit non-toxicity and excellent biocompatibility, thus being widely used in fluorescent biological markers [66,67] and biomedical adhesives [68]. In flexible field emission devices, one-dimensional (1D) SiC nanostructures show enhanced field emission performance due to their high aspect ratio [69]. Wu et al. [70] first reported the photoluminescence (PL) properties of SiC nanoparticles, laying a foundation for their applications in wavelength conversion and anti-reflection coatings of solar cells [71]. In addition, SiC is a wide-bandgap semiconductor with abundant color

center defects, whose atomic-scale defects can serve as qubits and single-photon sources. Owing to the long coherence time of these color center spin states at room temperature and their emission wavelength range close to the communication window, SiC has become an ideal platform for high-sensitivity quantum sensing of physical quantities such as magnetic field, electric field, and temperature [72]. For example, Fisher et al. [73] achieved high-resolution alternating current quantum magnetic resonance sensing using a single silicon vacancy defect in a commercial 4H-SiC substrate, with a spectral resolution of 0.33 Hz, demonstrating that CMOS-compatible SiC has the potential to realize scalable nanoscale quantum sensors.

To achieve the above functions, the precise preparation and engineering of color center defects are crucial. Currently, researchers introduce color centers into SiC using methods such as ion implantation, electron/neutron irradiation, femtosecond laser writing, and focused ion beam, and stabilize the charge states of defects through high-temperature annealing. Among them, femtosecond laser and focused ion beam technologies can achieve precise positioning of single defects at the nanoscale, which are highly controllable defect engineering methods at present [74]. For instance, Kraus et al. [75] realized site-specific silicon vacancy array generation without subsequent annealing in high-purity 4H-SiC via focused proton beam. The optimized SiC color centers can achieve a spin coherence time of tens to hundreds of microseconds at room temperature, laying a foundation for the development of device-level qubits.

In the field of power electronics and smart grids, SiC power devices have significantly improved system energy efficiency and supported higher voltages and frequencies due to their high thermal conductivity, high breakdown field strength, and fast switching characteristics [76]. Currently, SiC MOSFETs and Schottky diodes have been widely used in electric vehicles, grid inverters, and industrial power supplies. For example, SiC devices have realized bidirectional energy transmission in on-board charging systems, enabling “vehicle-grid” interaction, which can not only charge the battery but also feed back to the grid during power outages. In renewable energy systems, the adoption of 2300 V SiC modules can replace the traditional three-level structure, simplifying the circuit and improving power density and energy conversion efficiency. As smart grids increasingly demand bidirectional power flow and rapid response, SiC technology will further promote the efficient integration of distributed energy and energy storage systems.

Meanwhile, breakthroughs are still needed in SiC wafer-level manufacturing. The production cost of SiC single crystals remains high, and residual defects and impurities still pose challenges for quantum applications. Studies have shown that isotope purification can effectively reduce nuclear spin noise, increasing the coherence time of silicon vacancy color centers at room temperature by more than an order of magnitude [77]. Therefore, high-purity, low-defect single-crystal SiC substrates are the key foundation for realizing high-performance quantum devices.

5. Summary and outlook

SiC features a covalent crystal structure and polytypism (e.g., 3C-, 4H-, and 6H-SiC), accompanied by exceptional properties including high temperature resistance (melting point >2700 °C), hardness (Mohs hardness 9.5), low thermal expansion coefficient (4.5×10^{-6} °C^{-1}), and a wide bandgap (2.2 eV for 3C-SiC). These characteristics render it a foundational material for extreme-environment applications and third-generation semiconductors. However, despite its extensive application prospects in extreme environments and high-voltage electronic devices, SiC industrialization

still faces multiple technical bottlenecks. For instance, dislocation defects such as micropipes and screw dislocations in single-crystal SiC wafers significantly degrade device stability and breakdown voltage. Meanwhile, the fabrication of large-sized wafers via CVD requires ultra-high temperatures exceeding 2500 °C and high-purity precursors, resulting in high energy consumption and costs.

In comparison, other wide bandgap semiconductors offer distinct performance-cost trade-offs: gallium nitride (GaN, Eg ≈ 3.4 eV) can be epitaxially grown on low-cost silicon substrates, making it suitable for high-frequency applications below 600 V and already widely utilized in fast-charging power supplies. Aluminum nitride (AlN, Eg ≈ 6.0 eV), despite exhibiting higher breakdown field strength and lower conduction loss, remains in the experimental research stage due to greater process complexity and higher costs. Overall, SiC is more applicable to ultra-high-voltage, high-power systems (e.g., traction inverters in electric vehicles, high-voltage converters in smart grids), whereas GaN is better suited for medium-low voltage, high-frequency applications (e.g., communication devices and mobile power supplies).

Challenges remain:

(1) Synthesis: difficulties exist in controlling impurities in micro/nanopowders and regulating their crystal orientation.

(2) Defects: dislocations (e.g., micropipes, stacking faults) are present in single-crystal SiC wafers, which impair device reliability.

(3) Mechanistic insights: the understanding of structure–property–environment coupling relationships in cross-domain applications remains incomplete.

Future directions:

(1) Quantum technology: engineering nitrogen-vacancy (NV) centers in SiC to develop high-temperature quantum sensors and solid-state qubits.

(2) Green synthesis: developing biomass-derived routes (e.g., from rice husks, sugarcane bagasse) and low-energy electrochemical methods to reduce the carbon footprint by over 30%.

(3) Energy systems: integrating SiC-based devices (MOSFETs, insulated gate bipolar transistors (IGBTs)) into smart grids and hybrid energy storage systems, with targets of >98% efficiency at switching frequencies >100 kHz and withstand voltages >10 kV.

With advancements in quantum engineering, materials genomics, and clean energy technologies, SiC is poised to evolve into a multifunctional platform, driving innovations in high-temperature electronics, quantum technologies, and carbon neutrality.

Use of AI tools declaration

The authors declare they have not used Artificial Intelligence (AI) tools in the creation of this article.

Author contributions

Dong Ao-Yi: formal analysis, writing—original draft; Liu Shi-Kai: conceptualization, methodology; Shen Shao-Yi: study design, methodology; Wang Jia-Lin: formal analysis, investigation; Liu Xin-Xin: formal analysis, investigation; Han Bi-Bo: literature search, investigation; Wu Song: literature search, investigation; Zheng Xin-Hua: formal analysis; Sun Ya-Guang: formal analysis.

Acknowledgments

This work was supported by the Science and Technology Program of Henan Province, China (Grant# 222102230034); Henan University of Technology High-level Talent Research Fund Project (Grant #31401596). We thank Lady L. P. Guo from the School of Foreign Languages at Henan University of Technology for help.

Conflict of interest

The authors declare no conflict of interest.

References

1. Yang F, Chen YH, Hai WX, et al. (2025) Research progress on high-thermal-conductivity silicon carbide ceramics. *Ceram Int* 51: 4095–4109. https://doi.org/10.1016/j.ceramint.2024.11.408
2. An QL, Chen J, Ming WW, et al. (2021) Machining of SiC ceramic matrix composites: A review. *Chin J Aeronaut* 34: 540–567. https://doi.org/10.1016/j.cja.2020.08.001
3. Yu Z, Lv X, Mao K, et al. (2020) Role of in-situ formed free carbon on electromagnetic absorption properties of polymer-derived SiC ceramics. *J Adv Ceram* 9: 617–628. https://doi.org/10.1007/s40145-020-0401-x
4. She X, Huang AQ, Lucía O, et al. (2017) Review of silicon carbide power devices and their applications. *IEEE Trans Ind Electron* 64: 8193–8205. https://doi.org/10.1109/TIE.2017.2652401
5. Wang YY, Dong S, Li XT, et al. (2022) Synthesis, properties, and multifarious applications of SiC nanoparticles: A review. *Ceram Int* 48: 8882–8913. https://doi.org/10.1016/j.ceramint.2021.12.208
6. Shi B, Ramones AI, Liu Y, et al. (2023) A review of silicon carbide MOSFETs in electrified vehicles: Application, challenges, and future development. *IET Power Electron* 16: 2103–2120. https://doi.org/10.1049/pel2.12524
7. Hsiao TC, Tsao S (2012) Synthesis and purification of silicon carbide powders for crystal growth. *Mater Sci Forum* 717–720: 37–40. https://doi.org/10.4028/www.scientific.net/MSF.717-720.37
8. Wang L, Hu XB, Xu XG, et al. (2007) Synthesis of high purity SiC powder for high-resistivity SiC single crystals growth. *J Mater Sci Technol* 23: 118–122. https://www.jmst.org/EN/Y2007/V23/I01/118
9. Singh S, Chaudhary T, Khanna G (2022) Recent advancements in wide band semiconductors (SiC and GaN) technology for future devices. *Silicon* 14: 5793–5800. https://doi.org/10.1007/s12633-021-01362-3
10. Kimoto T, Cooper JA (2014) *Fundamentals of Silicon Carbide Technology: Growth, Characterization, Devices and Applications*, New York: John Wiley & Sons. https://doi.org/10.1002/9781118313534
11. Wang JC, Liu P, Fu XZ, et al. (2009) Relationship between oxygen defects and the photocatalytic property of ZnO nanocrystals in nafion membranes. *Langmuir* 25: 1218–1223. https://doi.org/10.1021/la803370z
12. Chen PC, Miao WC, Ahmed T, et al. (2022) Defect inspection techniques in SiC. *Nanoscale Res Lett* 17: 30. https://doi.org/10.1186/s11671-022-03672-w

13. Soltys LM, Mironyuk IF, Mykytyn IM, et al. (2023) Synthesis and properties of silicon carbide. *Phys Chem Solid Stat* 24: 5–16. https://doi.org/10.15330/pcss.24.1.5-16
14. Morkoc H, Strite S, Gao GB, et al. (1994) Large-band-gap SiC, III-V nitride, and II-VI ZnSe-based semiconductor device technologies. *J Appl Phys* 76: 1363–1398. https://doi.org/10.1063/1.358463
15. El Mendili Y, Orberger B, Chateigner D, et al. (2020) Insight into the structural, elastic and electronic properties of a new orthorhombic 6O-SiC polytype. *Sci Rep* 10: 7562. https://doi.org/10.1038/s41598-020-64415-4
16. Bhatnagar M, Baliga BJ (1993) Comparison of 6H-SiC, 3C-SiC, and Si for power devices. *IEEE Trans Electron Devices* 40: 645–655. https://doi.org/10.1109/16.199372
17. Eom JH, Kim YW, Song IH, et al. (2007) Microstructure and properties of porous silicon carbide ceramics fabricated by carbothermal reduction and subsequent sintering process. *Mater Sci Eng A* 464: 129–134. https://doi.org/10.1016/j.msea.2007.03.076
18. Presser V, Nickel KG (2008) Silica on silicon carbide. *Crit Rev Solid State* 33: 1–99. https://doi.org/10.1080/10408430701718914
19. Goldberg Y, Levinshtein M, Rumyantsev S (2001) Silicon carbide, In: Levinshtein ME, Rumyantsev SL, Shur MS, *Properties of Advanced Semiconductor Materials: GaN, AIN, InN, BN, SiC, SiGe*, New York: John Wiley & Sons, 93–146.
20. Morkoç H, Strite S, Gao GB, et al. (1994) Large-band-gap SiC, III-V nitride, and II-VI ZnSe-based semiconductor device technologies. *J Appl Phys* 6: 1363–1398. https://doi.org/10.1063/1.358463
21. Papanasam E, Kumar BP, Chanthini B, et al. (2022) A comprehensive review of recent progress, prospect and challenges of silicon carbide and its applications. *Silicon* 14: 12887–12900. https://doi.org/10.1007/s12633-022-01998-9
22. Lavric H, Zajec P, Drobnic K, et al. (2025) Challenges for large-scale deployment of WBG in power electronics. *Inf Midem-J Microelectron Electron Compon Mater* 55: 3–23. https://doi.org/10.33180/InfMIDEM2025.101
23. Sun KD, Wang TT, Gong WB, et al. (2022) Synthesis and potential applications of silicon carbide nanomaterials/nanocomposites. *Ceram Int* 48: 32571–32587. https://doi.org/10.1016/j.ceramint.2022.07.204
24. Gao SB, Jiang SN, Wang S, et al. (2020) Recycle of silicon slurry cutting waste to prepare high purity SiC by salt-assisted carbothermic reduction. *J Clean Prod* 272: 122566. https://doi.org/10.1016/j.jclepro.2020.122566
25. Lu PF, Jin ZH, Cui YB, et al. (2021) Effect of raw material particle size on synthesis of silicon carbide. *CIESC J* 72: 2300–2308. https://doi.org/10.11949/0438-1157.20200981
26. Mukasyan AS, Lin YC, Rogachev AS, et al. (2013) Direct combustion synthesis of silicon carbide nanopowder from the elements. *J Am Ceram Soc* 96: 111–117. https://doi.org/10.1111/jace.12107
27. Kirakosyan H, Nazaretyan K, Amirkhanyan N, et al. (2024) A novel pathway of solution combustion synthesis of silicon carbide and SiC based composite whiskers. *AIP Conf Proc* 2989: 040009. https://doi.org/10.1063/5.0189204
28. Han LJ, Chen SL, Li HH, et al. (2024) Rapid and inexpensive synthesis of liter-scale SiC aerogels. *Nat Commun* 15: 6959. https://doi.org/10.1038/s41467-024-51278-w

29. Han LJ, Zhang HK, Yang X, et al. (2025) Combustion co-synthesis of nano SiC and purified Si_3N_4 powders by coupling strong and weak exothermic reactions. *Ind Chem Mater* 12. https://doi.org/10.1039/d5im00191a
30. Karim GA, Ghosh A, Rao R, et al. (2021) Biomorphic SiC: Porous SiC and ultrafine SiC powder formation through biomimicking route. *Adv Appl Ceram* 120: 24–31. https://doi.org/10.1080/17436753.2020.1842106
31. Cui H, Zheng Y, Ma J, et al. (2017) Effect of different silicon sources on rattan-based silicon carbide ceramic prepared by one-step pyrolysis. *J Wood Sci* 63: 95–103. https://doi.org/10.1007/s10086-016-1594-z
32. Amirthan G, Udayakumar A, Prasad VVB, et al. (2009) Synthesis and characterization of Si/SiC ceramics prepared using cotton fabric. *Ceram Int* 35: 967–973. https://doi.org/10.1016/j.ceramint.2008.04.014
33. Alweendo ST, Johnson OT, Shongwe MB, et al. (2019) Synthesis, optimization and characterization of silicon carbide (SiC) from rice husk. *Procedia Manuf* 35: 962–967. https://doi.org/10.1016/j.promfg.2019.06.042
34. Do TKK, Nguyen CT, Huynh NM (2024) Effect of temperature on the ability to synthesize SiC from rice husks. *Mater Res Express* 11: 055510. https://doi.org/10.1088/2053-1591/ad4981
35. Li JW, Tian JM, Dong LM (2000) Synthesis of SiC precursors by a two-step sol-gel process and their conversion to SiC powders. *J European Ceram Soc* 20: 1853–1857. https://doi.org/10.1016/s0955-2219(00)00055-8
36. Najafi A, Golestani-Fard F, Rezaie HR, et al. (2021) Sol-gel synthesis and characterization of SiC–B_4C nano powder. *Ceram Int* 47: 6376–6387. https://doi.org/10.1016/j.ceramint.2020.10.218
37. Cerneaux S, Xiong X, Simon GP, et al. (2007) Sol–gel synthesis of SiC–TiO_2 nanoparticles for microwave processing. *Nanotechnology* 18: 055708. https://doi.org/10.1088/0957-4484/18/5/055708
38. Xie W, Möbus G, Zhang SW (2011) Molten salt synthesis of silicon carbide nanorods using carbon nanotubes as templates. *J Mater Chem* 21: 18325–18330. https://doi.org/10.1039/c1jm13186a
39. Wang FC, Zhao L, Fang W, et al. (2015) Synthesis and characterization of silicon carbide nanowires from lignin-phenolic resin and silicon powder with an in-situ formed molten salt as catalyst. *New Carbon Mater* 30: 222–229. https://doi.org/10.1016/s1872-5805(15)60187-1
40. Pang ZY, Li X, Zhang XQ, et al. (2022) Molten salt electrosynthesis of silicon carbide nanoparticles and their photoluminescence property. *Trans Nonferrous Met Soc China* 32: 3790–3800. https://doi.org/10.1016/s1003-6326(22)66058-8
41. Fedorov R, Lederle F, Li MJ, et al. (2021) Formation of titanium nitride, titanium carbide, and silicon carbide surfaces by high power femtosecond laser treatment. *ChemPlusChem* 86: 1231–1242. https://doi.org/10.1002/cplu.202100118
42. Wu Q, Yu S, Zhong H, et al. (2018) Preparation of silicon carbide coating by chemical vapor deposition by using hexamethyldisilylamine precursor. *Surf Coat Tech* 334: 78–83. https://doi.org/10.1016/j.surfcoat.2017.11.017.
43. Bertran E, Viera G, Martínez E, et al. (2000) Surface analysis of nanostructured ceramic coatings containing silicon carbide nanoparticles produced by plasma modulation chemical vapour deposition. *Thin Solid Films* 377: 495–500. https://doi.org/10.1016/S0040-6090(00)01374-2

44. Zhang WL, Chen Y, Dong YM, et al. (2025) Advances in preparation techniques for high-purity silicon carbide ceramics. *Int J Appl Ceram Technol* 22: e70012. https://doi.org/10.1111/ijac.70012
45. Herzallah H, Elsayd A, Shash A, et al. (2020) Effect ofcarbon nanotubes (CNTs) and silicon carbide (SiC) on mechanical properties of pure Al manufactured by powder metallurgy. *J Mater Res Technol-JMRT* 9: 1948–1954. https://doi.org/10.1016/j.jmrt.2019.12.027
46. Dong X, Ren Y, Wang Y, et al. (2024) Research progress of pressureless sintered silicon carbide bulletproof ceramic materials. *Bull Chin Ceram Soc* 43: 2225–2240. https://doi.org/10.1080/17436753.2019.1574285
47. Liu QA, Han WB, Han JC (2010) Influence of SiCnp content on the microstructure and mechanical properties of ZrB_2-SiC nanocomposite. *Scr Mater* 63: 581–584. https://doi.org/10.1016/j.scriptamat.2010.06.005
48. Mikociak D, Rudawski A, Blazewicz S (2018) Mechanical and thermal properties of C/C composites modified with SiC nanofiller. *Mater Sci Eng A-Struct Mater Prop Microstruct Process* 716: 220–227. https://doi.org/10.1016/j.msea.2018.01.048
49. Efe GC, Ipek M, Zeytin S, et al. (2012) An investigation of the effect of SiC particle size on Cu-SiC composites. *Compos Part B Eng* 43: 1813–1822. https://doi.org/10.1016/j.compositesb.2012.01.006
50. Zhu JW, Jiang WM, Li GY, et al. (2020) Microstructure and mechanical properties of SiCnp/Al6082 aluminum matrix composites prepared by squeeze casting combined with stir casting. *J Mater Process Technol* 283: 116699. https://doi.org/10.1016/j.jmatprotec.2020.116699
51. Bazzar M, Ghaemy M (2013) 1,2,4-Triazole and quinoxaline based polyimide reinforced with neat and epoxide-end capped modified SiC nanoparticles: Study thermal, mechanical and photophysical properties. *Compos Sci Technol* 86: 101–108. https://doi.org/10.1016/j.compscitech.2013.07.005
52. Duong-Viet C, Ba H, El-Berrichi Z, et al. (2016) Silicon carbide foam as a porous support platform for catalytic applications. *New J Chem* 40: 4285–4299. https://doi.org/10.1039/c5nj02847g
53. Silva CG, Passos FB, da Silva VT (2019) Influence ofthe support on the activity of a supported nickel-promoted molybdenum carbide catalyst for dry reforming of methane. *J Catal* 375: 507–518. https://doi.org/10.1016/j.jcat.2019.05.024
54. Elamin MM, Muraza O, Malaibari Z, et al. (2015) Microwave assisted growth of SAPO-34 on β-SiC foams for methanol dehydration to dimethyl ether. *Chem Eng J* 274: 113–122. https://doi.org/10.1016/j.cej.2015.03.118
55. Park KS, Son M, Park MJ, et al. (2018) Adjusted interactions of nickel nanoparticles with cobalt-modified $MgAl_2O_4$-SiC for an enhanced catalytic stability during steam reforming of propane. *Appl Catal A-Gen* 549: 117–133. https://doi.org/10.1016/j.apcata.2017.09.031
56. Liu CY, Yu DW, Kirk DW, et al. (2017) Electromagnetic wave absorption of silicon carbide based materials. *RSC Adv* 7: 595–605. https://doi.org/10.1039/c6ra25142k
57. Hu W, Wang L, Wu Q, et al. (2014) Preparation, characterization and microwave absorption properties of bamboo-like β-SiC nanowhiskers by molten-salt synthesis. *J Mater Sci Mater Electron* 25: 5302–5308. https://doi.org/10.1007/s10854-014-2305-4

58. Chiu SC, Yu HC, Li YY (2010) High electromagnetic wave absorption performance of silicon carbide nanowires in the gigahertz range. *J Phys Chem C* 114: 1947–1952. https://doi.org/10.1021/jp905127t
59. Hou Y, Cheng LF, Zhang YI, et al. (2017) Electrospinning of Fe/SiC hybrid fibers for highly efficient microwave absorption. *ACS Appl Mater Interfaces* 9: 7265–7271. https://doi.org/10.1021/acsami.6b15721
60. Ojha GP, Kang GW, Kuk YS, et al. (2022) Silicon carbide nanostructures as potential carbide material for electrochemical supercapacitors: A review. *Nanomaterials* 13: 150. https://doi.org/10.3390/nano13010150
61. Abdel Maksoud MIA, Fahim RA, Shalan AE, et al. (2020) Advanced materials and technologies for supercapacitors used in energy conversion and storage: A review. *Environ Chem Lett* 19: 375–439. https://doi.org/10.1007/s10311-020-01075-w
62. Perez-Chavez M, Esquivel-Castro TA, Rodriguez-Gonzalez C, et al. (2025) A Graphene/SiO_2/MnO/Graphene-SiC composite electrode printed on tinned steel for the fabrication of supercapacitors with high energy density. *J Mater Sci-Mater Electron* 36: 1670. https://doi.org/10.1007/s10854-025-15751-6
63. Liu YW, Li GH, Huan L, et al. (2024) Advancements in silicon carbide-based supercapacitors: Materials, performance, and emerging applications. *Nanoscale* 16: 504–526. https://doi.org/10.1039/d3nr05050e
64. Alper JP, Kim MS, Vincent M, et al. (2013) Silicon carbide nanowires as highly robust electrodes for micro-supercapacitors. *J Power Sources* 230: 298–302. https://doi.org/10.1016/j.jpowsour.2012.12.085
65. Gu L, Wang YW, Fang YJ, et al. (2013) Performance characteristics of supercapacitor electrodes made of silicon carbide nanowires grown on carbon fabric. *J Power Sources* 243: 648–653. https://doi.org/10.1016/j.jpowsour.2013.06.050
66. Beke D, Szekrényes Z, Pálfi D, et al. (2013) Silicon carbide quantum dots for bioimaging. *J Mater Res* 28: 205–209. https://doi.org/10.1557/jmr.2012.296
67. Botsoa J, Lysenko V, Géloën A, et al. (2008) Application of 3C-SiC quantum dots for living cell imaging. *Appl Phys Lett* 92: 173902. https://doi.org/10.1063/1.2919731
68. Attalla R, Ling CSN, Selvaganapathy PR (2018) Silicon carbide nanoparticles as an effective bioadhesive to bond collagen containing composite gel layers for tissue engineering applications. *Adv Healthcare Mater* 7: 1701385. https://doi.org/10.1002/adhm.201701385
69. Zhang XN, Chen YQ, Xie ZP, et al. (2010) Shape and doping enhanced field emission properties of quasialigned 3C-SiC nanowires. *J Phys Chem C* 114: 8251–8255. https://doi.org/10.1021/jp101067f
70. Wu XL, Fan JY, Qiu T, et al. (2005) Experimental evidence for the quantum confinement effect in 3C-SiC nanocrystallites. *Phys Rev Lett* 94: 026102. https://doi.org/10.1103/PhysRevLett.94.026102
71. Benfadel K, Kaci S, Hamidouche F, et al. (2021) Development of an antireflection layer using a lds based on β-SiC nanoparticles. *Silicon* 13: 1751–1763. https://doi.org/10.1007/s12633-020-00551-w
72. Zhang G, Cheng Y, Chou JP, et al. (2020) Material platforms for defect qubits and single-photon emitters. *Appl Phys Rev* 7: 031308. https://doi.org/10.1063/5.0006075

73. Fisher P, Zappacosta A, Fuhrmann J, et al. (2025) High-resolution nanoscale AC quantum sensing in CMOS compatible SiC. *Nano Lett* 25: 11626–11631. https://doi.org/10.1021/acs.nanolett.5c02515
74. Capan I (2025) Defects in silicon carbide as quantum qubits: Recent advances in defect engineering. *Appl Sci* 15: 5606. https://doi.org/10.3390/app15105606
75. Kraus H, Simin D, Kasper C, et al. (2017) Three-dimensional proton beam writing of optically active coherent vacancy spins in silicon carbide. *Nano Lett* 17: 2865–2870. https://doi.org/10.1021/acs.nanolett.6b05395
76. Roccaforte F, Alquier D, Kimoto T, et al. (2024) Silicon carbide materials and devices: Power electronics and innovative applications. *Mater Sci Semicond Process* 182: 108675. https://doi.org/10.1016/j.mssp.2024.108675
77. Lekavicius I, Myers-Ward RL, Pennachio DJ, et al. (2022) Orders of magnitude improvement in coherence of silicon-vacancy ensembles in isotopically purified 4H-SiC. *PRX Quantum* 3: 010343. https://doi.org/10.1103/PRXQuantum.3.010343

AIMS Press